A small bispecific protein selected for orthogonal affinity purification

Tove Alm, Louise Yderland, Johan Nilvebrant, Anneli Halldin, Sophia Hober

Biotechnology Journal

A small bispecific protein selected for orthogonal affinity purification

Journal:	*Biotechnology Journal*
Manuscript ID:	biot.201000041.R1
Wiley - Manuscript type:	Research Article
Date Submitted by the Author:	12-Apr-2010
Complete List of Authors:	Alm, Tove; Proteomics, Biotechnology Yderland, Louise; Proteomics, Biotechnology Nilvebrant, Johan; Proteomics, Biotechnology Halldin, Anneli; Proteomics, Biotechnology Hober, Sophia; Proteomics, Biotechnology
Primary Keywords:	Bispecific binder
Secondary Keywords:	Orthogonal purification
Keywords:	Phage display, ABD, Z domain

Research Article ((8636 words))

A small bispecific protein selected for orthogonal affinity purification

Tove Alm, Louise Yderland, Johan Nilvebrant, Anneli Halldin, and Sophia Hober*

School of Biotechnology, Department of Proteomics, Royal Institute of Technology, AlbaNova University Center, Stockholm, Sweden

Key words: Bispecific binder, orthogonal purification, phage display, ABD, Z domain

*Corresponding Author

Sophia Hober, Professor

AlbaNova University Center

KTH, School of Biotechnology, Proteomics

106 91 Stockholm, Sweden

Fax: +46 5537 8481 Tele: +46 5537 8330

Email: sophia.hober@biotech.kth.se

ABD	Albumin binding domain
ABD*	Stabilized albumin binding domain
Amp	Ampicillin
BSA	Bovine serum albumin
CD	Circular dichroism
Cml	Chloramphenicol
CV	Column volume
HBS-EP	HEPES buffered saline
HSA	Human serum albumin
IMAC	Immobilized metal affinity chromatography
PBS	Phosphate buffered saline
PBST	Phosphate buffered saline supplemented with tween
PBSTB 5%	PBST supplemented with 5% bovine serum albumin
SDS-PAGE	Sodium dodecyl sufate polyacrylamide gel electrophoresis
SPA	Staphylococcal protein A
TSB	Tryptic soy broth
TYE	Tryptone yeast extract
Z_2 domain	Dimeric Z domain

Abstract

A novel protein domain with dual affinity has been created by randomization and selection. The small alkali stabilized albumin binding domain (ABD*) used as scaffold to construct the library, has affinity to human serum albumin (HSA) and is constituted of 46 amino acids of which 11 were randomized. To achieve a dual binder, the binding site of the inherent HSA-affinity was untouched and the randomization was made on the opposite side of the molecule. Despite its small size and randomization of almost 1/4th of its amino acids a bifunctional molecule, ABDz1, with ability to bind to both HSA and the Z_2 domain/protein A was successfully selected using phage display. Moreover the newly selected variant showed improved affinity for HSA compared to the parental molecule. This novel protein domain has been characterized regarding secondary structure and affinity to the two different ligands. The possibility for affinity purification on two different matrices has been investigated using the two ligands, the HSA-matrix and the protein A-based, MabSelect SuRe-matrix, and the new protein domain was purified to homogeneity. Furthermore, gene fusions between the new domain and three different target proteins with different characteristics were made. To take advantage of both affinities, a purification strategy referred to as orthogonal affinity purification using two different matrices was created. Successful purification of all three versions could efficiently be carried out by the orthogonal affinity purification strategy.

1 Introduction

Due to the high cost in producing and purifying proteins the production steps as well as the purification of the target protein need to be optimized. For high throughput production and purification of many proteins in parallel, general methods without the need for individual optimization are necessary. Recombinant techniques allow efficient production of target proteins and affinity chromatography offers a selective purification method. In order to achieve effective purification for a wide range of different proteins, a selective purification tag can be used. Different affinity interactions have been exploited for this purpose, e.g. enzyme-substrate, protein-metal, protein-carbohydrate, or protein-protein [1]. Depending on the choice of interaction partners the cost and complexity of the purification conditions will vary. The choice of affinity tag can also influence the amount of produced protein, its solubility, stability and function. A small tag is less likely to interfere with the target protein and its further applications. Another important aspect is that the tag should be robust and fold easily regardless of target protein. In order to achieve a target protein with high purity usually more than one purification step is necessary. To increase the selectivity of the purification method and thus enhance the purity of the sample, an orthogonal purification strategy would be beneficial. In classical orthogonal purification design, the succeeding separation characteristics are distinct from each

other, utilizing different characteristics of the proteins. Here we introduce the term orthogonal affinity purification. Endowing one purification tag with more than one useable affinity would increase the efficiency of the purification. The two binding surfaces in the small bispecific tag could be used for subsequent purification without any target specific optimization.

A small protein domain, historically used as affinity tag for protein purification, is the albumin binding domain (ABD) [2]. ABD is a three helical bundle [3] derived from the Streptococcal protein G [4]. To render this domain further usable in affinity purification it has been engineered into a variant denoted ABD* with increased resistance to alkaline conditions [5]. Hence, cleaning in place of the equipment including the affinity matrix with ABD* coupled as ligand is possible. To gain more information about the protein domain, directed mutagenesis was used to locate the albumin-binding site. It was concluded to be positioned mainly in the second helix [6]. This finding was further supported by structural investigations, using NMR and X-ray crystallography [7, 8]. Also triple alanine mutants were made in helix one and three at positions pointing away from the suggested binding site showing retained or increased binding to human serum albumin (HSA) [6]. Thus indicating that positions pointing away from the HSA binding surface would be possible to randomize to create a library that renders selection of new binders with retained affinity to HSA possible. Due to the improved characteristics of ABD* and its ability to bind HSA, it was chosen as scaffold when creating the phage display library.

Another protein also frequently used for protein purification, both as affinity ligand

and as purification tag, is the Staphylococcal protein A (SPA) [9]. The high selectivity has made protein A matrices commonly used for antibody purification [10] and due to the availability of affinity matrices with protein A as ligand, one of the domains responsible for IgG-binding was chosen as target in the phage display selection.

Here we, for the first time, present a strategy that makes it possible to select small proteinaceous binders capable to selectively bind two different proteins. Moreover the possibility of purifying a selected and characterized variant from the ABD*-library using two different affinity matrices was investigated. Finally, the selected domain was introduced in the N-terminus of three different target proteins and utilized as affinity tag in two succeeding purification steps.

2 Materials and methods

2.1 Bacterial strains and oligonucleotides

For recombinant- and phage work the *Escherichia coli* (*E. coli*) strain RRIΔM15 was used [11]. The recombinant DNA techniques used were carried out essentially as described by Sambrook et al. [12]. Oligonucleotides for the library construction were synthesized at SGS (Scandinavian Gene Synthesis, Köping, Sweden). All other primers were synthesized at MWG (MWG-BIOTECH AG, Ebersberg, Germany).

DNA restriction enzymes were bought from MBI Fermentas (MBI Fermentas, Vilnius, Lithuania). Protein production was carried out in *E. coli* strain Rosetta(DE3) (Novagen, Merck KGaA, Darmstadt, Germany) and all protein purifications were carried out using an ÄKTAExplorer (GE Healthcare, Uppsala, Sweden).

2.2 Library construction

The phagemid vector pML was constructed from pKN [13] by introduction of an *EcoR*I-site and a dummy fragment using restriction sites *Mlu*I and *Xho*I. pML was restricted using *EcoR*I and *Xho*I and the restricted vector was separated on a 1% agarose gel and extracted from the gel using QIAquick Gel Extraction Kit (QIAGEN, Solna, Sweden). The library was assembled using oligonucleotides ABDlibCod3 and ABDlibRev3 having complementary regions in the part encoding helix two. The DNA-fragments were hybridized and extended using six temperature cycles with AmpliTaq Gold (Applied Biosystems, Foster City, CA, USA), purified using QIAquick PCR Purification Kit (QIAGEN) and restricted using *EcoR*I and *Xho*I. After separation and extraction from a 3% low melt agarose gel the purified vector and fragment were ligated using T4 DNA Ligase (New England BioLabs, Boston, MA, USA). To remove contaminating proteins the ligation mixture was phenol-chloroform extracted and thereafter ethanol precipitated. The plasmids were transformed into electrocompetent RRIΔM15 using Bio-Rad Gene Pulser (Bio-Rad Laboratories, Hercules, CA, USA) to yield a final library size of ~10^7 members.

2.3 Analysis of the ABD-library*

The library was analyzed by PCR amplification and DNA sequencing was performed on an ABI 3700 DNA Sequencer (Applied Biosystems).

To assess the retainment of HSA-binding in the library two rounds of phage selection against HSA were performed. HSA (Sigma-Aldrich, Steinheim, Germany) was biotinylated using EZ-Link Sulfo-NHS-LC-Biotin (Pierce, IL, USA) according to the manufacturer's recommendation. The selections were carried out as described in section 2.4 with a target concentration of 1 μM with the exception that cycle 1 was performed with the target protein captured on paramagnetic beads during the binding step.

A western blot was done on phage stocks eluted from cycle 1 and 2 to analyze the enrichment of HSA-binders from the initial library. As a positive control cell lysate with the parental ABD* was included. The samples were reduced and analyzed by sodium dodecyl sulphate polyacrylamide gel electrophoresis (SDS-PAGE) on a 4-12% gradient NuPAGE Novex Bis-Tris gel (Invitrogen, Paisely, Scotland). After separation the proteins were transferred to a nitrocellulose membrane (Bio-Rad Laboratories) using an XCell II™ Blot Module (Invitrogen). The membrane was blocked with phosphate buffered saline supplemented with tween (50 mM phosphate, 100 mM NaCl, pH 7.2, 0.1% Tween 20) (PBST) also containing 1% gelatin. The membranes were incubated with biotinylated HSA (120 nM) for 1 h, followed by

washing (PBST), incubation with the secondary peroxidase-conjugated streptavidin (DakoCytomation, Glostrup, Denmark) (0.6 g/l diluted 1:5000), and a final washing step. Detection was carried out using a CCD-camera (Bio-Rad) with SuperSignal West Dura Extended Duration Substrate (Pierce) according to the manufacturer's protocol.

To investigate the degree of truncated pIII in relation to full length on the phage surface, another western blot analysis was done as described above but detection was carried out using a primary mouse antibody recognizing pIII (Nordic Biosite, Täby, Sweden) (0.5 g/l diluted 1:1000) and a secondary peroxidase-conjugated rabbit antibody (Sigma-Aldrich) (diluted 1:5000). The relative intensities of the bands were compared using QuantityOne software (BioRad).

2.4 Selection

Four rounds of selection in solution against a dimeric Z domain (Z_2 domain) [14] were performed. All tubes used in the selection were protein LoBind tubes (Eppendorf, VWR International, Stockholm, Sweden) blocked with PBST supplemented with 5% bovine serum albumin (BSA) (Sigma-Aldrich) (PBSTB 5%). Streptavidin-coated or REGEN beads coated with neutravidin according to manufacturer's recommendations (Dynal Biotech, Oslo, Norway) were used for preselection and selection. Beads were washed in 2*500 µl PBST and blocked with 500 µl PBSTB 5%. Four series (A, B, C, and D) with different target concentration

were performed and to increase the stringency of each cycle the number of washes and amount of Tween 20 in the washing buffer (PBST supplemented with 3% BSA) was increased for each cycle, table 1. PBS was used in the last wash of each cycle. For each round of selection a new phage stock was prepared by infection with helper phage M13KO7 (New England BioLabs), followed by polyethylene glycol and sodium chloride (PEG/NaCl) precipitation resulting in phage titers of 10^{11}-10^{12} cfu/ml. Each round of selection started with a negative selection using the corresponding blocked paramagnetic beads. The supernatant from this step was moved to a new tube and mixed with the biotinylated Z_2 domain at varying concentrations, table 1, and incubated for two hours at room temperature (RT). The binding phages were captured on 0.5 mg of paramagnetic beads and washed as described above. For elution, incubation with 500 µl of 0.05 M glycin-HCl pH 2.2 for 10 minutes at RT was performed. After elution the pH was adjusted with 450 µl PBS and 50 µl 1 M Tris-HCl pH 8.0. The eluate was mixed with log phase RRIΔM15 and incubated at 37°C for 30 minutes. Thereafter the cells were spread on Tryptone Yeast Extract (TYE) agar plates (15 g/l agar, 3 g/l NaCl, 10 g/l tryptone and 5 g/l yeast extract), supplemented with 2% glucose and 100 mg/l ampicillin (Amp) (Sigma-Aldrich) and incubated at 37°C over night. The cells were resuspended in tryptic soy broth (TSB, 30 g/l) (Merck, Darmstadt, Germany). A fraction of the cell suspension was used to create a new phage stock. Elution titers and number of phages introduced in each cycle were determined by infection of log phase RRIΔM15.

2.5 Cloning

Cloning of ABD-variants*

Colonies from cycle three and four were randomly picked from agar plates supplemented with 100 mg/l Amp for PCR screening and sequencing. Three constructs were chosen for further investigation; ABDz1, ABDz83, ABDz86 (ABDzx, x=1, 83, 86). The ABD* library fragments were amplified by PCR, using Phusion High Fidelity DNA polymerase (New England BioLabs). The cystein in ABDz1 was replaced by a serine using primer ABDz1C25S and PCR-mutagenesis to create ABDz1C25S. The fragments were purified before restriction as described sin section 2.2. The expression vector pHis (containing a T7-promoter, a His-tag, and a kanamycin resistance gene) and the fragments ABDzx and ABDz1C25S were cleaved with the restriction enzymes *EcoRI* and *XhoI*. The purified fragments were ligated with pHis using T4 DNA Ligase (New England BioLabs) resulting in pHisABDzx and pHisABDz1C25S. A dimeric version of ABDz1C25S was created using primers ABDdimerCod and ABDdimerRev with pHisABDz1C25S as template, resulting in a fragment with flanking *XhoI* restriction sites. The purified fragment and pHisABDz1C25S were restricted with *XhoI* and purified. The linear vector was dephosphorylated using Antarctic Phosphatase (New England BioLabs). Subsequent ligation resulted in pHisABDz1C25SDim.

Cloning of target proteins in fusion with ABDz1

DNA fragments containing only ABDz1 were made by PCR, using primers ABDz1Not1 and ABDz1Nco1, incorporating restriction sites Nco1 and Not1. The restriction enzymes were used to cleave the purified PCR fragment and vectors containing different target proteins; pZbABP141377, pZbABPHT875, and pZbABPHT2375 [15]. Ligation of vector and ABDz1-fragment was performed at RT using T4 DNA ligase (New England BioLabs) giving pABDz1-141377, pABDz1-HT875 and pABDz1-HT2375. The plasmids were sequence verified.

2.6 Protein production

Protein production was essentially performed according to [15]. After protein production for 18 hours, the cell suspensions were gently harvested (2400 g, 8 min, 4°C) and pellets were frozen for later use.

2.7 Protein purification of His_6-tagged ABD-variants*

The frozen pellets were resuspended in 25 ml running buffer (50 mM sodium phosphate, 6 M Urea, 300 mM NaCl, pH 8.0) and cells were disrupted by sonication (Vibra cell; Sonics and materials, Inc., Danbury, CT, USA) at 60% amplitude and 1.0/1.0 pulses for 3 minutes. Before loading on a 1 ml Talon resin column (Clontech Laboratories, Inc., Mountain View, CA, USA) the samples were centrifuged (35000 g, 20 min, 4°C) and filtered (0.45 µm). The column was equilibrated with 5 column volumes (CV) of running buffer and 20 ml of sample was loaded. After washing with

20 CV running buffer bound proteins were eluted with elution buffer (50 mM NaAc, 6 M Urea, 100 mM NaCl, 30 mM HAc, pH 4.5).

2.8 Protein analysis

The eluted proteins were analyzed by SDS-PAGE using a NuPAGE Novex Bis-Tris 4-12% gradient gel stained with GelCode Blue Stain Reagent (Pierce). NAP10 columns (GE Healthcare) were used for buffer exchange to HEPES buffered saline (10 mM HEPES, 150 mM NaCl, 3.4 mM EDTA and 0.05% surfactant P20, pH 7.4) (HBS-EP). Protein concentration was determined by absorbance measurements at 280 nm and amino acid analysis.

2.9 Biosensor analysis

Real-time biospecific interaction analysis between the selected variants and the target protein, the Z_2 domain, as well as its original binding partner, HSA, was performed on a Biacore 2000 instrument (GE Healthcare). The Z_2 domain was immobilized (~130 RU) by thiol coupling through a C-terminal Cys and HSA was immobilized (~2500 RU) by amine coupling onto the dextran layer of a CM5 chip according to the manufacturer's instructions. All analytes were diluted in HBS-EP, and filtered through a 0.45 µm filter. ABD* and IgG were included in all analyses as controls. After every injection the surfaces were regenerated using 15 mM HCl. In the initial study each variant (ABDzx, ABDz1C25S and ABDz1C25SDim) was diluted to ~500

nM and injected over all surfaces at 50 µl/min. For kinetic studies a new chip was made with an immobilization level of ~200 RU and ~2000 RU on the Z_2-surface and HSA-surface respectively. ABD* and ABDz1C25S were analyzed on the HSA-surface and ABDz1 on the Z_2-surface in concentrations ranging from 10 nM to 1000 nM at a flow rate of 50 µl/min. The association rate constant (k_a), the dissociation rate constant (k_d), and the dissociation equilibrium constant (K_D) were estimated using BIAevaluation 3.2 software (Biacore).

2.10 Circular dichroism

Analysis of secondary structure was performed using a J-810 spectropolarimeter (JASCO, Tokyo, Japan). All samples were diluted to approximately 0.22 mg/ml except ABD* that was diluted to 0.05 mg/ml in PBS. The samples were scanned in a 1 mm cell from 250 nm to 195 nm at a speed of 100 nm/min. An average from five scans was calculated. Using the same sample the thermal stability was also investigated by heating the sample from 20°C to 90°C using a temperature slope of 5°C/min. The circular dichorism (CD) signal at 221 nm was detected. Thereafter a new CD spectrum was performed as previously described to investigate if the protein regained its secondary structure.

2.11 Protein purification using HSA sepharose

The frozen pellets were resuspended in 25 ml running buffer (25 mM Tris–HCl, 200

mM NaCl, 1 mM EDTA, 0.05% Tween 20, pH 8.0) and supernatant containing protein lysate was prepared as described in section 2.7. The protein lysates were loaded on a column with 1 ml HSA Sepharose. The column was equilibrated with 10 CV of running buffer and 25 ml of the sample was loaded. After washing with 5 CV running buffer and 5 CV washing buffer (5 mM NH_4Ac, pH 5.5) the bound proteins were eluted with 0.5 M HAc, pH 2.8. The protein concentration in the eluted fractions was determined by absorbance measurements at 280 nm. The eluted peaks were analyzed using SDS-PAGE as described in section 2.8. To compare the binding capacity of ABD* and ABDz1 to the HSA sepharose, equal amounts of previously purified protein were loaded onto the column and purified as described above. In the orthogonal purification setup, the two protein fractions with the highest absorbance from the SuRe purification step were pooled and pH was adjusted to 7.5 before loading on the HSA sepharose and purified as described above.

2.12 Protein purification using MabSelect SuRe

The frozen pellets were thawed and resuspended in 25 ml running buffer (20 mM phosphate, 150 mM NaCl, pH 7.2) and the supernatants containing protein lysates were prepared as described in section 2.7. The protein solution was loaded on a 1 ml HiTrap MabSelect SuRe column (GE Healthcare). The column was equilibrated with 5 CV of running buffer and 20 ml of sample was loaded. After washing with 5 CV of running buffer the proteins were eluted with 0.2 M HAc, pH 3.3. In the orthogonal

purification setup the two protein fractions with the highest absorbance from the HSA purification step were pooled and pH was adjusted to 7.5 before loading on the SuRe matrix and purified as described above. To investigate if it was possible to achieve effective purification also under reducing conditions one sample was treated with 50 mM DL-Dithiothreitol (DTT) (Sigma-Aldrich) at 37°C for 30 minutes before filtration and loading onto the column and thereafter the described purification scheme was used. In an attempt to find milder elution the samples were eluted using 0.2 M HAc at pH 3.3, pH 4.0 and pH 4.5. The fractions of the eluted peaks were pooled and analyzed as described in section 2.8. When purifying fusion proteins using the SuRe matrix 0.2 M HAc at pH 3.3 was used as elution buffer.

3. Results

3.1 Rationale for the design of the library

Here we present a novel phage display library of ~10^7 variants constructed to create a possibility to achieve small protein molecules that with high selectivity are able to bind two different target molecules. For construction of the library, a small and stable molecule with inherent and selective binding to a protein target, was desired. Due to improved characteristics [5] and the inherent binding property, ABD* was chosen as scaffold for the library. In an earlier mutational study [6] it was also shown that

despite mutations of nine amino acids in helix one and three, at positions distant from the suggested binding site, the HSA-binding was retained or even improved. Therefore these nine amino acids in helix one and three and two additional amino acids, at the end of helix one and helix three respectively, were chosen for randomization when building the library (Fig. 1a). The amino acids were randomized using NNK-degeneracy coding for all 20 amino acids and the amber stop (TAG) using 32 different codons. A visualization of the protein domain is shown in figure 1b where the three helices are shown as ribbons and in figure 1c the molecular surface is presented.

3.2 Analyses of the unbiased ABD-library*

To verify that the library was randomized in the correct positions and without bias for certain amino acids, 150 clones were sequenced. Approximately 93% of the selected clones were full-length library members with correct inserts. The remaining 7% were plasmids without insert and these clones were omitted in the sequencing reaction. The amino acid occurrence in the randomized positions of the full-length clones was compared to the theoretically expected occurrence of each amino acid. The distribution of each amino acid was found to be close to the theoretical value (data not shown).

To investigate if the HSA binding was retained, a western blot was performed on phage stocks from selections against HSA. ABD* was included in the western blot as

a positive control. A faint band can be seen in the lane with the naïve ABD*-library, and the intensity of the band is increased after each selection cycle (Fig. 2a). This confirms that the HSA-binding is retained in a large part of the represented protein molecules despite randomization of almost 25% of the amino acids in the small ABD* domain. The presence of truncated pIII-ABDlib in comparison with full-length pIII encoded by the phagemide was also investigated by western blot. In the original library 11% of the expressed pIII was the truncated (library) variant. After the first and second selection cycle against HSA the subset of truncated pIII-ABDlib increased to 17% and 37%, respectively, as determined by image analysis on western blot data, indicating enrichment of phages expressing truncated pIII in fusion with randomized protein domains (data not shown).

3.3 Selection

Isolation of Z_2-binders from the ABD*-library was achieved using phage display in-vitro selection technology. After four rounds of biopanning against the Z_2 domain, the same sequence was identified in all sequenced clones, ABDz1 (Fig. 2b). To encounter additional variants, clones from the third round of biopanning were sequenced. Of the 80 clones sequenced 84% were identical with the sequence found after cycle four, ABDz1. Two additional sequences appeared once each, ABDz83 and ABDz86. When sequencing clones from selection cycle two, ABDz1 was found only once (corresponding to less than 1% of the sequenced clones). The three variants,

ABDz1, ABDz83, and ABDz86, have low sequence homology in the randomized regions and all three were selected for further characterization.

3.4 Purification and analyses of ABD-variants*

The identified candidates were recloned into an expression vector containing the T7 promoter [16] and an N-terminal hexahistidyl purification tag [17]. After expression of the proteins in Rosetta, the cells were lysed and the His-tagged ABD*-variants were purified to homogeneity by immobilized metal affinity chromatography (IMAC).

Biosensor analysis was used to verify the binding between the selected variants and the target molecules, the Z_2 domain and HSA. The three variants, ABDz1, ABDz83, and ABDz86, were diluted to ~500 nM and the capacity to bind both the Z_2 domain and HSA was evaluated. The results showed that all three variants had retained HSA binding and that one of the three variants, ABDz1, possessed Z_2-binding as well (Fig. 3a and 3b). Hence, ABDz1 was chosen for further studies as it had the desired dual binding capacity and had the fastest on-rate when binding to HSA. Of the 11 positions randomized in ABDz1 two amino acids were conserved compared to the parental sequence; arginine in position 29 and tyrosine in position 34. Interestingly, a cysteine has been introduced in position 25 enabling disulfide formation between the molecules. Both lysines were exchanged to histidines, also basic amino acids, but with lower pKa. All acidic amino acids (positions 22, 30 and 58) were exchanged for

uncharged amino acids. The substitution in position 30 introduced a glycine in helix one (Fig. 1b and 2b). In total, all mutations resulted in an increase in theoretical pI from 5.8 to 6.4 and the net charge at neutral pH was decreased from -5 to -2.

By SDS-PAGE analysis it was concluded that ABDz1 appears as almost 100% homodimer due to intermolecular disulfide bridge formation (data not shown). To assess the importance of the dimerization for the binding to the Z_2 domain and HSA, the ABDz1 was further engineered by replacing the cysteine in position 25 by a serine creating a molecule denoted ABDz1C25S. To investigate the possible avidity effects and as a comparison to the dimer formed through the disulfide bridge a dimeric variant of ABDz1C25S was also created by head-to-tail dimerisation, ABDz1C25SDim. This construct excludes the N-terminal linker region of one ABDz1C25S, and therefore the molecular weight will be 13.3 kDa whereas it is 14.4 kDa for the dimeric ABDz1.

Surface plasmon resonance was used to compare the binding of the four protein molecules, ABDz1, ABDz1C25S, ABDz1C25SDim, and ABD*, to HSA. The concentrations were adjusted so that the number of available binding sites should be equal in all samples. All three novel constructs showed faster on-rate than ABD*, and ABDz1 had slower off-rate than all others (Fig. 3c). Avidity effects could be seen both for the genetic dimer, ABDz1C25SDim and the dimer formed by the cysteines in ABDz1 since these dimers showed higher apparent affinity than the corresponding monomer, ABDz1C25S. The dimers have similar affinity and the difference in response can be explained by the difference in molecular weight between the two

protein constructs (dimer of ABDz1 14.4 kDa and ABDz1C25SDim 13.3 kDa). It was also investigated if ABDz1 could retain the Z_2-binding after exchanging the cysteine for a serine but only ABDz1 showed affinity to the Z_2 domain (Fig. 3d).

Kinetic studies were performed to investigate the binding of ABD* and ABDz1C25S to HSA. To be able to use a one-to-one binding algorithm when calculating the binding constants, ABDz1C25S was used instead of the dimer-forming ABDz1. Due to the identical amino acids in the HSA-binding surface of the protein domains, the HSA affinities of a monomeric ABDz1 and ABDz1C25S would be very similar. The measured values for ABD* correspond well to earlier published data [5]. ABDz1C25S has approximately the same off-rate as ABD* but a faster on-rate and therefore the calculated dissociation equilibrium constant is slightly stronger, low nano molar, for ABDz1C25S (Table 2). A similar comparison for the binding to the Z_2 domain is less appropriate since dimerization of ABDz1 is crucial for Z_2-binding. However, kinetic analysis of the ABDz1 binding to the Z_2 domain using a one-to-one model gave an apparent K_D of low micro molar (Table 2).

Using circular dichroism the structural contents of the ABD* variants were determined. The structural characteristics of the selected variants were compared to ABD* which is a three-helical bundle as determined by NMR [3], and the high alpha-helicity is also confirmed by circular dichroism [5]. The curves from the CD analyses showed that despite a retained α-helical secondary structure, the signals were much lower than for the parental ABD*-molecule (data not shown). Hence, the alpha helical content in the new molecule is much lower than that in ABD*. Also the

modified variant, ABDz1C25S has less α-helicity than the parental domain (data not shown). Furthermore the thermal stability was investigated by comparing the curves before and after heating the sample. No change could be detected indicating that the molecules were able to refold and regain their structure.

3.5 Protein purification using the inherent affinities

An effective path to increase the purity of a proteinaceous target molecule is to purify it in an orthogonal way and take advantage of different characteristics when planning the purification strategy. Here we have investigated the possibility of purifying the bispecific ABDz1 on two different affinity matrices. The first purification column used contained HSA sepharose. The two proteins, ABD* and ABDz1, were successfully purified from cell lysate using this matrix. To assess the efficiency in the binding, ABDz1 was compared to ABD* by purifying equal amounts of protein in subsequent purifications. The eluted peak for ABD* was smaller due to low absorbance at 280 nm since the protein contains no tryptophan (Fig. 4a). SDS-PAGE analysis of loaded and eluted sample from the purification showed that equal amounts of protein were loaded on the column and that the matrices were able to capture all loaded protein in both cases (Fig. 4b). Hence, the mutated variant, ABDz1, and ABD* possess similar capacity to bind to the HSA sepharose.

To investigate if ABDz1 could be purified on MabSelect SuRe, a protein A-derived matrix, cell lysate was loaded on the column and captured protein was eluted using

pH 3.3 (Fig. 4c). This confirmed that the Z_2-binding capability introduced into ABDz1 enabled purification on MabSelect SuRe. Different elution conditions were used to investigate if a less harsh buffer than pH 3.3 was possible to use for elution of ABDz1 from the SuRe matrix. The target protein was eluted in comparable amounts when using pH 3.3 and pH 4.0, but at pH 4.5 a minor amount of the protein was eluted (Fig. 4c). When cleaning the column with pH 3.3 the majority of the loaded target protein was released (Fig. 4c). Analysis with SDS-PAGE confirmed amount and purity of the eluted target protein. Thus the pH of the elution buffer can be raised to 4.0 and still effective elution is accomplished.

To assess the importance of the disulfide bridge formed between the ABDz1 molecules for its binding to the Z_2-domain, DTT-treated sample was loaded onto the MabSelect SuRe matrix. Successful purification could not be achieved, possibly due to the reduced disulfide bridge (data not shown).

3.6 Protein purification using an orthogonal purification strategy

To challenge the usability of ABDz1 as purification tag, three different proteins with dissimilar characteristics (Table 3) were genetically fused with the gene encoding ABDz1 giving fusion proteins with the new binding domain in the N-terminus. The three fusion proteins and the sole tag were produced in *E. coli* and thereafter purified in two chromatographic steps. In the first purification step a column with HSA matrix was used and the purification efficiency was therefore dependent on the capacity of

the tag to bind to HSA. The eluted peaks were collected and a sub fraction of each peak was analyzed by SDS-PAGE. The rest of the eluted material was loaded on the protein A derived matrix, MabSelect SuRe, and the eluted fractions were also analyzed using SDS-PAGE. Moreover, it was investigated if the two matrices could be used in reverse order with comparable result. The orthogonal affinity purification principle was applied as described above on the three fusion proteins. This time the first purification was carried out on the MabSelect SuRe marix followed by HSA sepharose chromatography. As can be seen in figure 5 a and b, a very pure product can be obtained regardless of the characteristics of the target protein since the interaction with the matrix only is dependent on the N-terminal purification domain. Orthogonal affinity purification using the two affinities in ABDz1 can successfully be applied regardless of the order in which the two affinities are used.

4. Discussion

A novel phage display library based on the improved ABD domain, ABD* (Fig. 1) has been created. The library was used for selection of binders towards the Z_2 domain. The objective was to isolate a molecule with dual binding capacities to be used as a highly specific tag in affinity chromatography. It was concluded that the library size was approximately 10^7 and the distribution of amino acids were found to be close to the theoretical values. In spite of the extensive randomization, 11 of the 46

amino acids, enrichment of HSA-binders from the ABD* library was possible (Fig. 2a).

Selection of Z_2-binders from the library resulted in three different constructs with low sequence homology. All three variants contained a cysteine in the middle or at the end of helix one resulting in dimers formed by the disulfide bridge. However, only one of them showed Z_2-binding, ABDz1 (Fig. 2b and 3b), and was therefore chosen for further studies. Biosensor analysis of the affinity constants for ABDz1 binding to the Z_2 domain immobilized on the chip surface using a monovalent model gave an apparent K_D value of 0.4 μM (Table 2). The indication of moderate affinity was not surprising due to the rather small size of the library (approximately 10^7 variants) [18]. The Z_2-affinity dependence of the dimerization as well as the avidity effect gained by the disulfide formation was investigated by replacing the cysteine with a serine, creating ABDz1C25S. From this mutant a genetic dimer without cysteins was created, ABDz1C25SDim. Unfortunately, neither ABDz1C25S nor ABDz1C25SDim did show any Z_2-binding indicating that the conformation formed by ABDz1 through the cystein-bridge is crucial for binding. The surface formed by the dimerisation is not easily mimicked with a genetic head-to-tail dimerisation, which is shown by the inability of ABDz1C25SDim to bind to the Z_2 domain. Sensorgrams acquired with HSA on the surface show that the stronger response seen for ABDz1 compared to ABDz1C25S (and ABD*) is mainly due to dimerisation since ABDz1C25SDim shows almost equally strong response as ABDz1 to HSA (Fig. 3c). The somewhat

higher response seen for ABDz1 compared to ABDz1C25SDim is probably caused by differences in molecular weight but also due to the slightly slower off-rate for ABDz1 (Fig. 3c). Presumably, this effect is due to a more favorable conformation formed by the dimer as well as avidity effects caused by the dual binding sites. A closer examination of the kinetic constants for ABDz1C25S and ABD* showed that there was almost no difference in the dissociation rate constant, k_d, whereas the association rate constant, k_a, was higher for ABDz1C25S, and thus the calculated dissociation equilibrium constant, K_D, was lower, than for ABD* (Table 2). The faster on-rate can possibly be explained by the substitutions at the randomized positions. At the randomized positions in ABDz1C25S all negative charges were replaced by uncharged amino acids and an uncharged position was exchanged with a positively charged amino acid resulting in a less negatively charged molecule than the parental ABD*. Since HSA has negative net charge at the conditions used in the analysis (-12) the faster on-rate determined could be due to a less negative net charge of ABDz1C25S (-2) as compared to ABD* (-5). A similar charge affected behavior has earlier been shown for other interaction pairs as well [19, 20]. When examining the structural content of ABDz1 and ABDz1C25S using CD, a curve shape indicating a-helicity was acquired (data not shown). However, the signal intensities were much lower than for ABD* showing that the selected variants had a lower alpha helical content. The substitution in position 30 introduced a glycine in helix one. Since glycine is known to have low propensity for alpha helical structures this amino acid could partly be responsible for the low helical content [21-23]. Also the histidines

acquired at the end of helix one and in the middle of helix three might destabilize the structure as histidine has a low helix-stability rank [24]. In positions 57 and 58 in the third helix two aromatic amino acids were found, which also could affect the α-helicity. Even though the variants showed a lower structural content than ABD* they demonstrated superior binding characteristics to HSA. Interestingly, some sequential similarity can be seen in the binding surface of Z_{SpA-1}, a randomized variant of the Z-domain with Z-binding ability [25, 26], and the randomized surface of ABDz1. Z_{SpA-1} was selected from a library of Z variants (Z_{lib}) using the Z domain as target [25]. When comparing the interaction surface of Z_{SpA-1} with ABDz1 by placing two ABDz1 molecules beside each other, helix one from the left molecule and helix three from the right creates an interaction surface similar to Z_{SpA-1}. This, together with our experimental data, indicates that dimerization of ABDz1 is not crucial to gain avidity effects, but rather that two molecules are needed for the correct interaction surface to be created. This also conveys that the apparent affinity should be evaluated by using the concentration of the dimer instead of the monomer and thereby resulting in an apparent affinity of 0.2 μM. It has not been possible to detect binding between ABDz1 and variants of the Z domain (selected from Z_{lib}) using surface plasmon resonance (data not shown) indicating that the binding interphase of ABDz1 to the Z domain is in the same area as for Z_{SpA-1}, but this remains to be further investigated.

The dual characteristics established in ABDz1 encouraged further experiments where

the two acquired affinities were used for protein purification (Fig. 4). Purifications of ABDz1 using HSA as ligand on a sepharose matrix were shown to be as effective as for ABD*. Since the affinity for the Z_2 domain was not as strong as for HSA, purification on the protein A-derived matrix, MabSelect SuRe, would be more challenging. However, the purification was successful and due to the moderate affinity for the Z_2 domain, a strategy with milder elution conditions could be established.

To challenge the new domain as an affinity tag in protein purification, three different target proteins were genetically fused to the affinity domain. Target proteins with different molecular weight and also different pI were chosen (Table 3) to evaluate if the tag was affected by the characteristics of the attached protein. When utilizing the bispecific affinity domain in a two-step chromatographic purification setup a very high degree of purity was achieved for the target proteins (Fig. 5). Hence, the constructed affinity domain showed usefulness in protein purification and the domain was able to effectively interact with the two different matrices regardless of the characteristics of the C-terminal target protein. Noteworthy is that the two affinity chromatography steps can be used in any order.

In many applications very pure and active molecules are essential. Using an orthogonal affinity purification strategy with two succeeding affinity purification steps will greatly enhance the purity of the final product. A purification system built

on a genetic fusion to a purification tag is mainly suited for protein purification in small to medium scale systems. The large benefit is the possibility for high throughput purification of a wide variety of target proteins with different characteristics without any target specific optimization. By knowing the characteristics of the fused purification domain all details regarding the purification setup can be planned in advance. The low pH necessary for the disruption of the interaction between the affinity domain and the ligand on the matrix might, may for some target proteins, be too harsh. This effect can in many cases be decreased remarkably by immediately increasing the pH of the eluted sample. For some downstream applications it is essential to remove the purification tag from the target protein. This can be done by e.g. on-column digestion and has previously been shown successful [27].

Here we, for the first time, have shown that a small molecule, consisting of only 46 amino acids, can be engineered to have dual affinities. Moreover, the domain could be expressed in *E. coli* in fusion to three different target proteins. All these proteins, as well as the domain itself, could efficiently be purified in a two-step affinity chromatographic setup giving very pure protein. The achieved data show that the novel purification tag is efficient and the orthogonal affinity purification strategy gives highly pure protein. Also the similar behavior of the three different target proteins purified here indicates that the tag is of general use regardless of the target protein.

Acknowledgement

The authors thank Professor Per-Åke Nygren for scientific discussions and advice. This project was funded by the Knut and Alice Wallenberg Foundation and the Swedish Research Council.

The authors have declared no conflict of interest.

5. References

[1] Hedhammar, M., Graslund, T., Hober, S. Protein engineering strategies for selective protein purification. *Chemical Engineering & Technology* 2005; *28*: 1315-1325.

[2] Nilsson, J., Stahl, S., Lundeberg, J., Uhlen, M. et al. Affinity fusion strategies for detection, purification, and immobilization of recombinant proteins. *Protein Expr Purif* 1997; *11*: 1-16.

[3] Kraulis, P. J., Jonasson, P., Nygren, P. A., Uhlen, M. et al. The serum albumin-binding domain of streptococcal protein G is a three-helical bundle: a heteronuclear NMR study. *FEBS Lett* 1996; *378*: 190-194.

[4] Olsson, A., Eliasson, M., Guss, B., Nilsson, B. et al. Structure and evolution of the repetitive gene encoding streptococcal protein G. *Eur J Biochem* 1987; *168*: 319-324.

[5] Gulich, S., Linhult, M., Nygren, P., Uhlen, M. et al. Stability towards alkaline conditions can be engineered into a protein ligand. *J Biotechnol* 2000; *80*: 169-178.

[6] Linhult, M., Binz, H. K., Uhlen, M., Hober, S. Mutational analysis of the interaction between albumin-binding domain from streptococcal protein G and human serum albumin. *Protein Sci* 2002; *11*: 206-213.

[7] Johansson, M. U., Frick, I. M., Nilsson, H., Kraulis, P. J. et al. Structure, specificity, and mode of interaction for bacterial albumin-binding modules. *The Journal of biological chemistry* 2002; *277*: 8114-8120.

[8] Lejon, S., Frick, I. M., Bjorck, L., Wikstrom, M. et al. Crystal structure and biological implications of a bacterial albumin binding module in complex with human serum albumin. *The Journal of biological chemistry* 2004; *279*: 42924-42928.

[9] Uhlen, M., Guss, B., Nilsson, B., Gatenbeck, S. et al. Complete sequence of the staphylococcal gene encoding protein A. A gene evolved through multiple duplications. *The Journal of biological chemistry* 1984; *259*: 1695-1702.

[10] Hober, S., Nord, K., Linhult, M. Protein A chromatography for antibody purification. *J Chromatogr B Analyt Technol Biomed Life Sci* 2007; *848*: 40-47.

[11] Ruther, U. pUR 250 allows rapid chemical sequencing of both DNA strands of its inserts. *Nucleic Acids Res* 1982; *10*: 5765-5772.

[12] Sambrook, J., Fritsch, E. F., Maniatis, T. Molecular Cloning: A Laboratory Manual. Cold Spring Harbor Laboratory Press, New York 1989.

[13] Nord, K., Nilsson, J., Nilsson, B., Uhlen, M. et al. A combinatorial library of an alpha-helical bacterial receptor domain. *Protein Eng* 1995; *8*: 601-608.

[14] Nilsson, B., Moks, T., Jansson, B., Abrahmsen, L. et al. A synthetic IgG-binding domain based on staphylococcal protein A. *Protein Eng* 1987; *1*: 107-113.

[15] Alm, T., Steen, J., Ottosson, J., Hober, S. High-throughput protein purification under denaturating conditions by the use of cation exchange chromatography. *Biotechnol J* 2007; *2*: 709-716.

[16] Studier, F. W., Moffatt, B. A. Use of bacteriophage T7 RNA polymerase to direct selective high-level expression of cloned genes. *J Mol Biol* 1986; *189*: 113-130.

[17] Hochuli, E., Bannwarth, W., Dobeli, H., Gentz, R. et al. Genetic Approach to Facilitate Purification of Recombinant Proteins with a Novel Metal Chelate Adsorbent. *Bio/Technology* 1988; *6*: 1321-1325.

[18] Griffiths, A. D., Williams, S. C., Hartley, O., Tomlinson, I. M. et al. Isolation of high affinity human antibodies directly from large synthetic repertoires. *Embo J* 1994; *13*: 3245-3260.

[19] Schreiber, G., Fersht, A. R. Rapid, electrostatically assisted association of proteins. *Nat Struct Biol* 1996; *3*: 427-431.

[20] Albeck, S., Schreiber, G. Biophysical characterization of the interaction of the beta-lactamase TEM-1 with its protein inhibitor BLIP. *Biochemistry* 1999; *38*: 11-21.

[21] Bishop, B., Koay, D. C., Sartorelli, A. C., Regan, L. Reengineering granulocyte colony-stimulating factor for enhanced stability. *The Journal of biological chemistry* 2001; *276*: 33465-33470.

[22] Hecht, M. H., Hehir, K. M., Nelson, H. C., Sturtevant, J. M. et al. Increasing and decreasing protein stability: effects of revertant substitutions on the

thermal denaturation of phage lambda repressor. *Journal of cellular biochemistry* 1985; *29*: 217-224.

[23] Pace, C. N., Scholtz, J. M. A helix propensity scale based on experimental studies of peptides and proteins. *Biophysical journal* 1998; *75*: 422-427.

[24] O'Neil, K. T., DeGrado, W. F. A thermodynamic scale for the helix-forming tendencies of the commonly occurring amino acids. *Science* 1990; *250*: 646-651.

[25] Nord, K., Gunneriusson, E., Ringdahl, J., Stahl, S. et al. Binding proteins selected from combinatorial libraries of an alpha-helical bacterial receptor domain. *Nat Biotechnol* 1997; *15*: 772-777.

[26] Wahlberg, E., Lendel, C., Helgstrand, M., Allard, P. et al. An affibody in complex with a target protein: structure and coupled folding. *Proc Natl Acad Sci U S A* 2003; *100*: 3185-3190.

[27] Hedhammar, M., Jung, H. R., Hober, S. Enzymatic cleavage of fusion proteins using immobilised protease 3C. *Protein Expr Purif* 2006; *47*: 422-426.

[28] Hedhammar, M., Stenvall, M., Lonneborg, R., Nord, O. et al. A novel flow cytometry-based method for analysis of expression levels in Escherichia coli, giving information about precipitated and soluble protein. *J Biotechnol* 2005; *119*: 133-146.

Legends to figures

Figure 1

A) The original sequence of the three-helical ABD* [5] used as scaffold when building the library. The 11 randomized positions are indicated by increased font size. Numbering according to [3]. The shaded areas represent helix 1, 2, and 3 (H1, H2, and H3).

B) and C) The three-dimensional structure of ABD* as determined by NMR [3], protein data bank entry 1GJT, modulated by YASARA, shown as ribbon structure with the randomized positions numbered in circles (B) and molecular surface (C). Dark areas represent the randomized positions.

Figure 2

A) Western blot performed on phage stock from selections against HSA showing pIIIABDlib (27 kDa), lane 1, 2, and 3. ABD* (7 kDa) is included as a positive control, lane 4. A faint band can be seen in lane 1 which represents the HSA-binding phages in the original library and an increased intensity of the band can be seen after each round of selection, lane 2 and 3. Lane 2 shows the phage stock after the first selection cycle and lane 3 is after the second selection cycle. This confirms that the HSA-binding is retained in the scaffold despite randomization of almost 1/4th of the amino acids. Marker (M) in kDa.

B) The sequences of the selected variants ABDz1, ABDz83, and ABDz86. Only ABDz1 shows affinity to the Z_2 domain. However, all three have retained HSA binding. Numbering according to [3]. The 11 mutated positions are indicated by increased font size. The shaded areas represent helix 1, 2, and 3 (H1, H2, and H3).

Figure 3

Sensorgrams from biospecific interaction analysis

A and B) Sensorgrams showing the binding of the selected ABD* variants to HSA (A) or the Z_2 domain (B): ABDz1 (black line), ABDz83 (grey line), and ABDz86 (light grey line) (500 nM). In (A) HSA was immobilized on the surface. All three selected variants, ABDz1, ABDz83, and ABDz86, show HSA-binding. In (B) the Z_2 domain was immobilized on the surface. One of the selected variants, ABDz1, shows Z_2-binding.

C and D) Sensorgrams showing the binding of ABD* and variants thereof to HSA (C) or the Z_2 domain (D): ABD* (black dashed line) (500 nM), ABDz1 (black line) (500 nM), ABDz1C25S (grey dashed line) (500 nM), and ABDz1C25SDim (grey line) (250 nM). The concentrations are adjusted so that an equal number of molecules are available in each sample. In (C) HSA was immobilized on the surface. ABDz1C25SDim shows almost equally strong response as ABDz1 to HSA indicating that avidity effects are responsible for the stronger response for ABDz1 compared to ABDz1C25S. In (D) the Z_2 domain was immobilized on the surface. The cysteine-containing variant, ABDz1, shows Z_2-binding but neither the cysteine-free monomer

nor the cysteine-free dimer does. Thus the conformation created by the cysteine-bridge seems to be essential for binding.

Figure 4

Chromatograms from ÄKTAExplorer and SDS-PAGE gels

A and B) Elution profile of ABD* (dashed line) and ABDz1 (solid line) purified on HSA sepharose using an ÄKTAExplorer. To investigate the capacity of the selected variant, ABDz1, to bind the HSA sepharose and compare the binding with the parental ABD*, similar amounts of purified protein were loaded and eluted with pH 2.8 in subsequent purifications. The loaded sample and eluted peaks were analyzed using SDS-PAGE. Approximately equal amounts of ABDz1 (7.4 kDa) and ABD* (7.1 kDa) were loaded (lane 1 and 3 respectively) and eluted (lane 2 and 4 respectively). Marker (M) in kDa.

C and D) Elution profile of ABDz1 purified on MabSelect SuRe using an ÄKTAExplorer. Three protein lysates were pooled and divided into three equal volumes and loaded on the column in three subsequent purifications. ABDz1 was eluted using three different elution conditions, pH 3.3 (black line), 4.0 (dashed line), and 4.5 (grey line). The target protein was eluted in comparable amounts for pH 3.3 and pH 4.0, but at pH 4.5 the elution of the target protein was less effective, peak 1 (P1). In the setup using elution buffer at pH 4.5 the remaining target protein was released when washing with a buffer at pH 3.3, peak 2 (P2). Analysis of the loaded sample and eluted peaks was done by SDS-PAGE. Identical samples of protein lysate

were loaded (lane 1) in all three setups and efficient elution of ABDz1 (7.4 kDa) was achieved at pH 3.3 (P1) (lane 2) and pH 4.0 (P1) (lane 3). At pH 4.5 the elution was less effective (P1) (lane 4) and the remaining protein was washed out with a buffer at 3.3 (P2) (lane 5). Marker (M) in kDa.

Figure 5

SDS-PAGE analysis of target proteins expressed in fusion with ABDz1

A) Lane 1-4 shows the protein lysates before purification. In lanes 5-8 results from the first purification step using HSA matrix are shown. In lanes 9-12 results from the second purification step by MabSelect SuRe is shown. Samples are loaded in the following order: ABDz1-141377, ABDz1-HT875, ABDz1-HT2375 and ABDz1.

B) Lane 1-3 shows protein lysates before purification. Lanes 4-6 show the results from the first purification step using MabSelect SuRe. Lanes 7-9 show the results from the second purification step, HSA purification. Samples are loaded in the following order: ABDz1-141377, ABDz1-HT875, and ABDz1-HT2375.

The molecular weight of respective protein is shown in table 3.

The orthogonal affinity purification setup using the bispecific ABDz1 gives very pure protein regardless of target protein fused to the tag. The two chromatographic steps can be used in any order.

Tables

Table 1

Biopanning by phage display

	A	B	C	D	Number of washes	Tween %
Cycle 1	100 nM			100 nM (N)	3	0.1
Cycle 2	80 nM	20 nM	80 nM	80 nM	5	0.2
Cycle 3	80 nM	20 nM	50 nM	50 nM (N)	7	0.3
Cycle 4	80 nM	20 nM	20 nM	20 nM	10	0.4

Four series (A, B, C, and D) of biopanning with different target concentration were performed in four cycles (1, 2, 3 and 4). To increase the stringency in every selection round, the number of washes and the amount of tween was increased in each cycle. Streptavidin coated beads have been used if not stated (N) for neutravidin.

Table 2

Kinetic constants from surface plasmon resonance measurements

	k_a (M^{-1} s^{-1})	k_d (s^{-1})	K_D (M)
ABD*	3.5E+04	1.4E-03	4.0E-08
ABDz1C25S	2.7E+05	1.3E-03	4.8E-09

Ligand: HSA

	k_a (M^{-1} s^{-1})	k_d (s^{-1})	K_D (M)
ABDz1	1.1E+04	3.9E-03	4.0E-07

Ligand: Z_2 domain

Data have been evaluated using an one-to-one model. Due to the dimerization of ABDz1 the values describe the apparent affinity.

k_a=association rate constant

k_d=dissociation rate constant

K_D=dissociation equilibrium constant

Table 3

Characteristics of the target and fusion proteins used for evaluation of the bispecific affinity protein domain as a purification tag.

	Target protein			Fusion product	
Name [a)]	**Uniprot** [b)]	**Mw**[c)] **[kDa]**	**Solubility Class**[d)]	**Mw**[c)] **[kDa]**	**pI**[e)]
141377	B7Z3I5	17.4	4	23.7	8.5
HT875	P01040	10.8	3	17.1	4.9
HT2375	P00740	8.9	5	15.2	6.8

Affinity tag, ABDz1: 6.3 kDa, pI 6.7

ABDz1 (including an N-terminal His_6-tag): 7.4 kDa, pI 6.4

[a)] The target protein represents a part of the Uniprot protein

[b)] http://www.uniprot.org

[c)] Mw = molecular weight

[d)] Solubility class of protein fragment with N-terminal His_6ABP [28]

[e)] pI = isoelectric point

167x17mm (150 x 150 DPI)

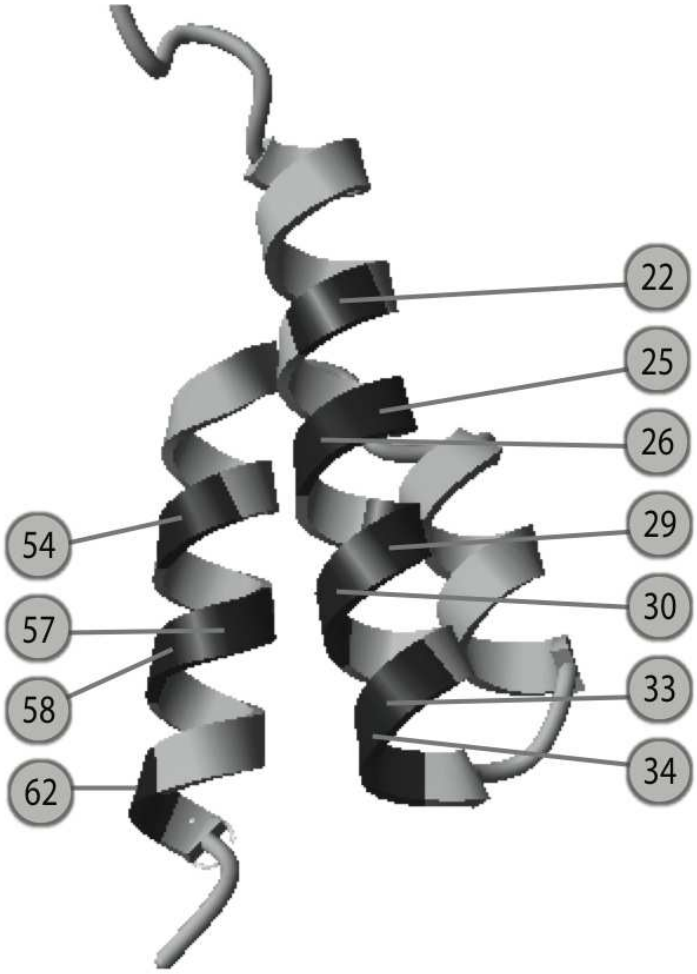

144x144mm (150 x 150 DPI)

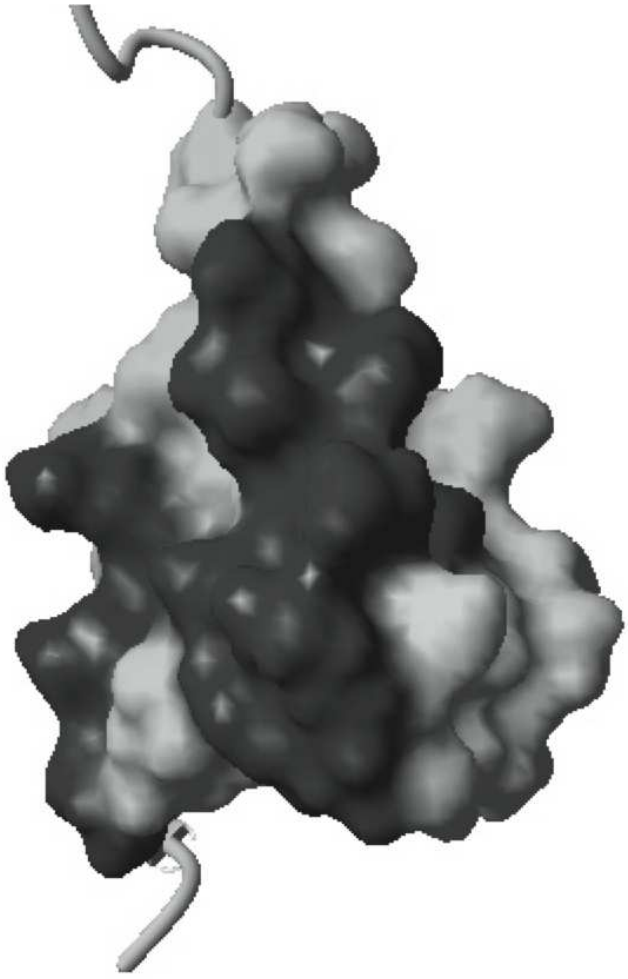

144x144mm (150 x 150 DPI)

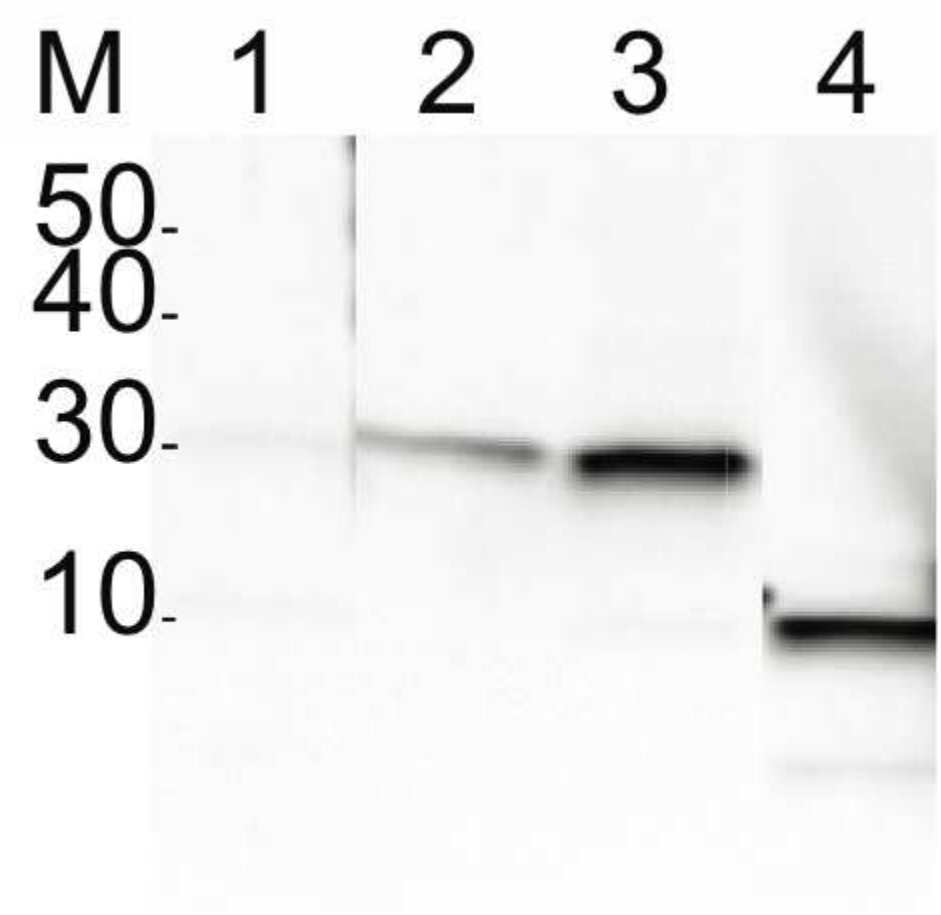

80x78mm (150 x 150 DPI)

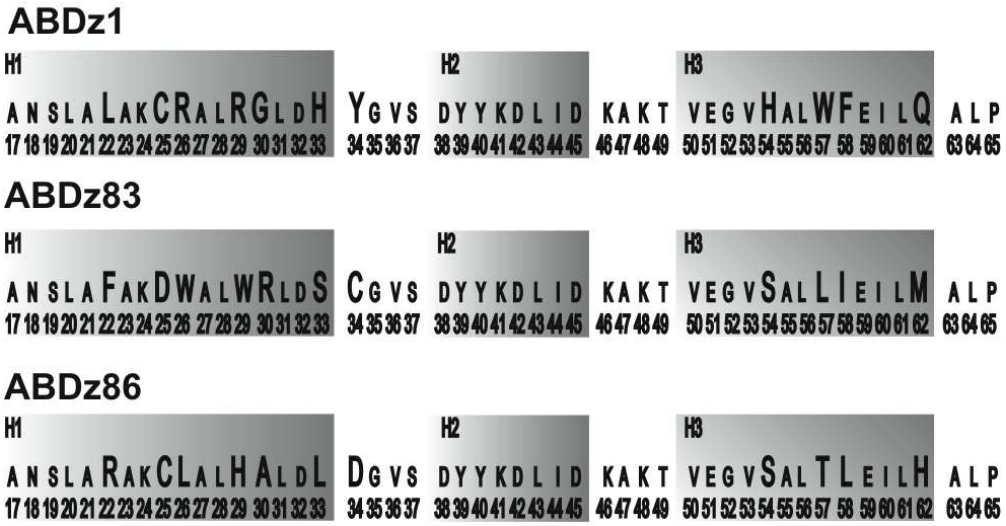

166x91mm (150 x 150 DPI)

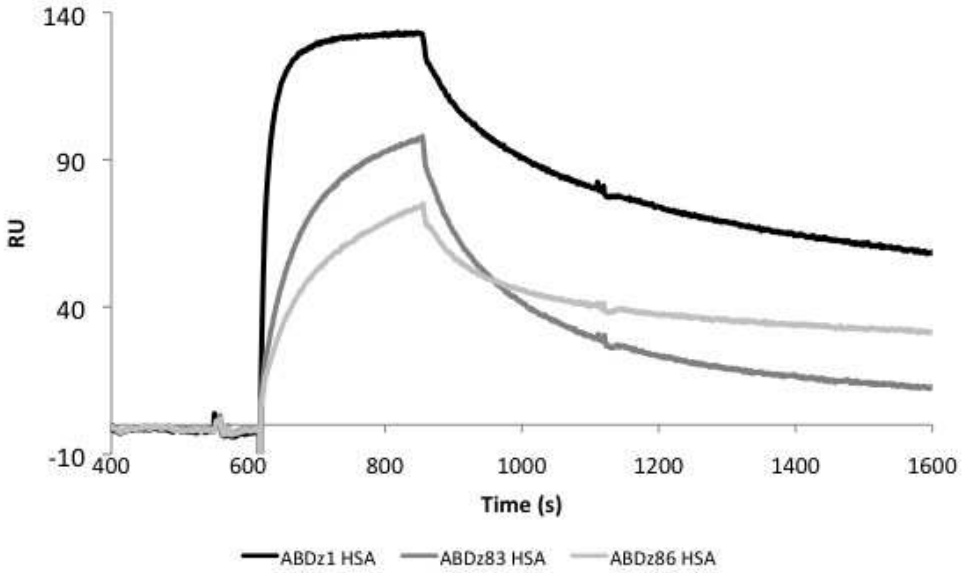

200x120mm (72 x 72 DPI)

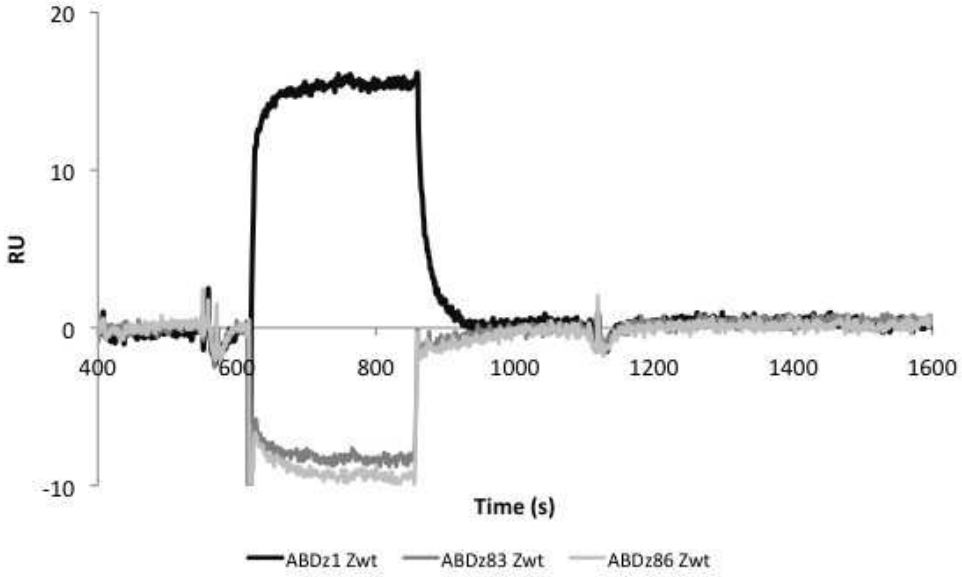

200x120mm (72 x 72 DPI)

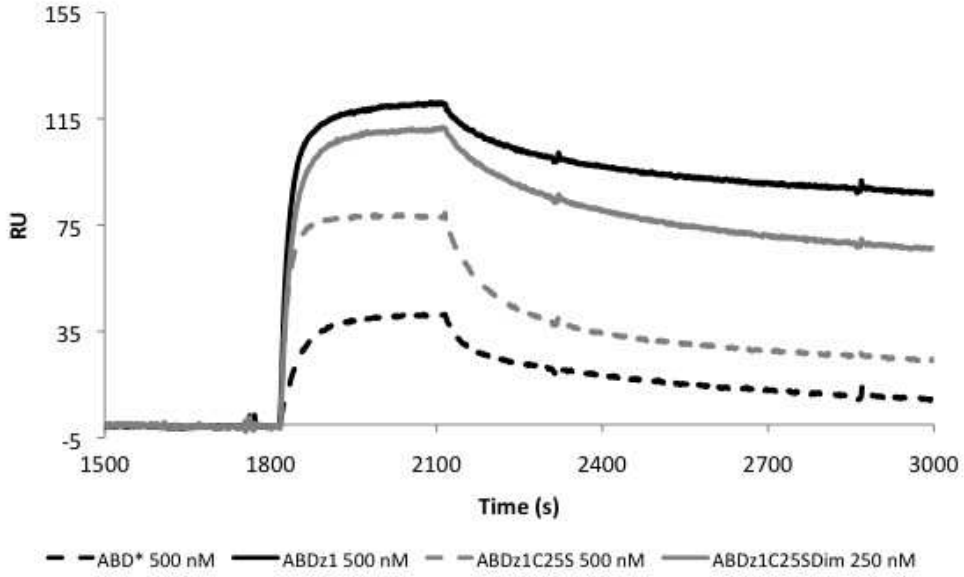

200x120mm (72 x 72 DPI)

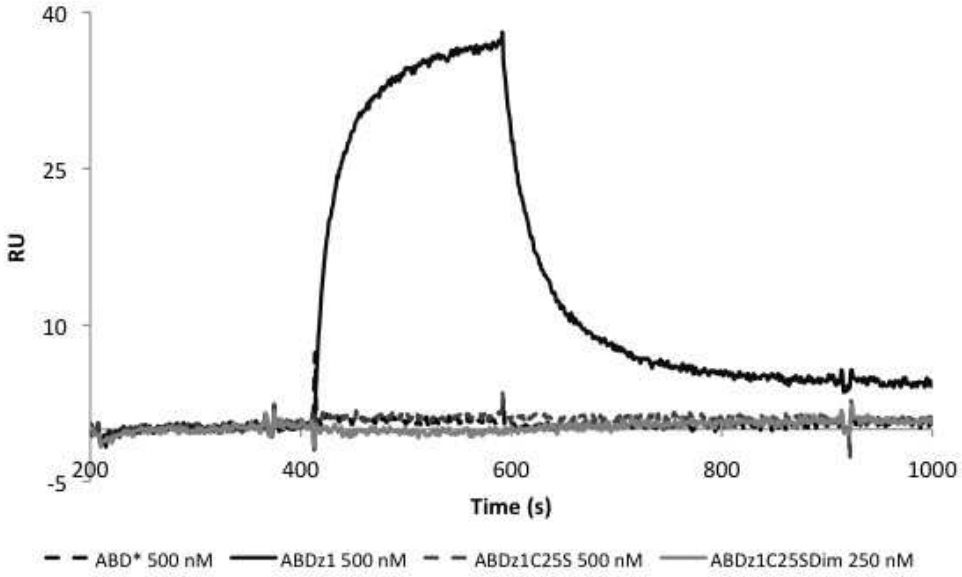

200x120mm (72 x 72 DPI)

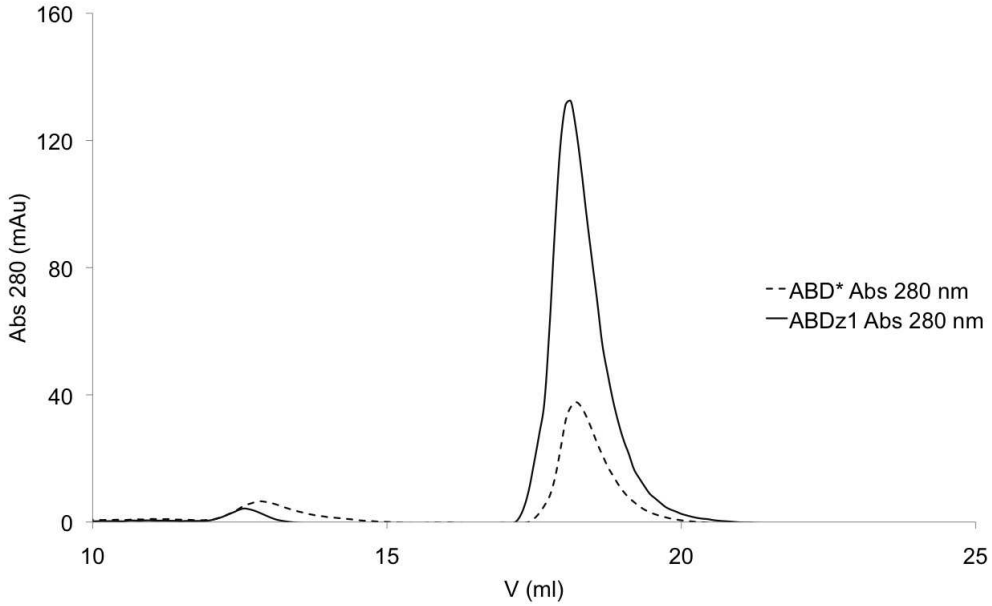

439x271mm (72 x 72 DPI)

67x66mm (150 x 150 DPI)

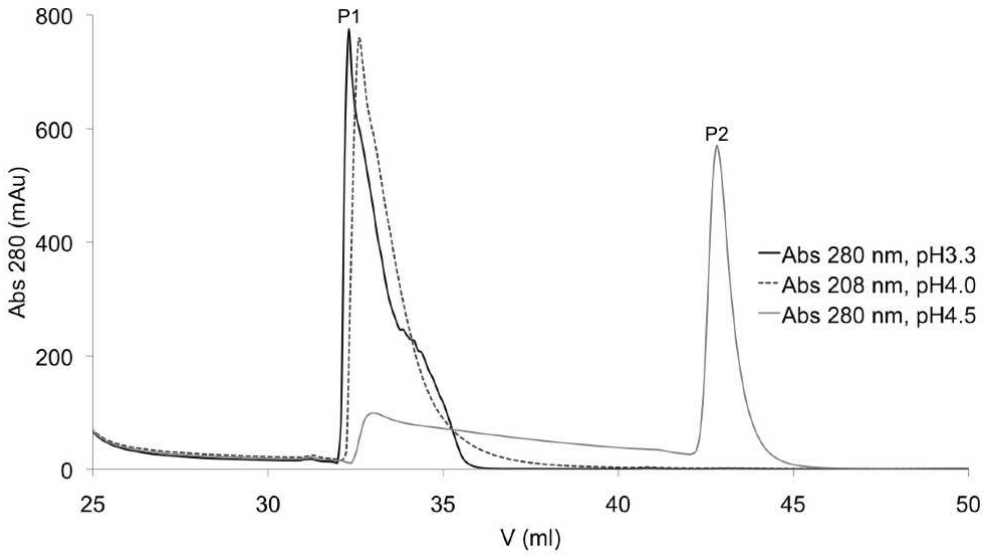

168x96mm (150 x 150 DPI)

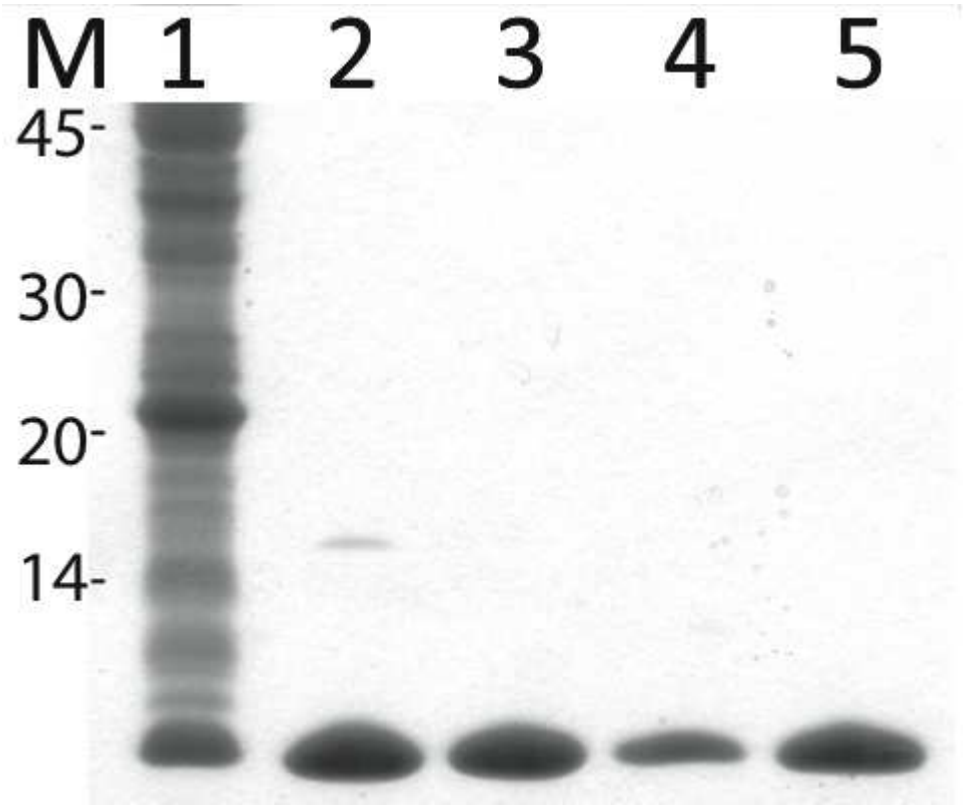

81x67mm (150 x 150 DPI)

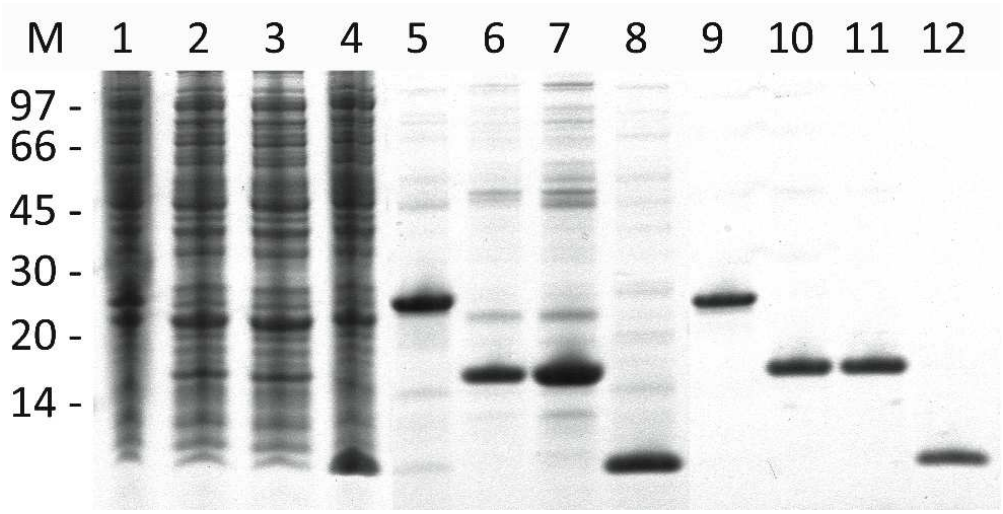

166x84mm (150 x 150 DPI)

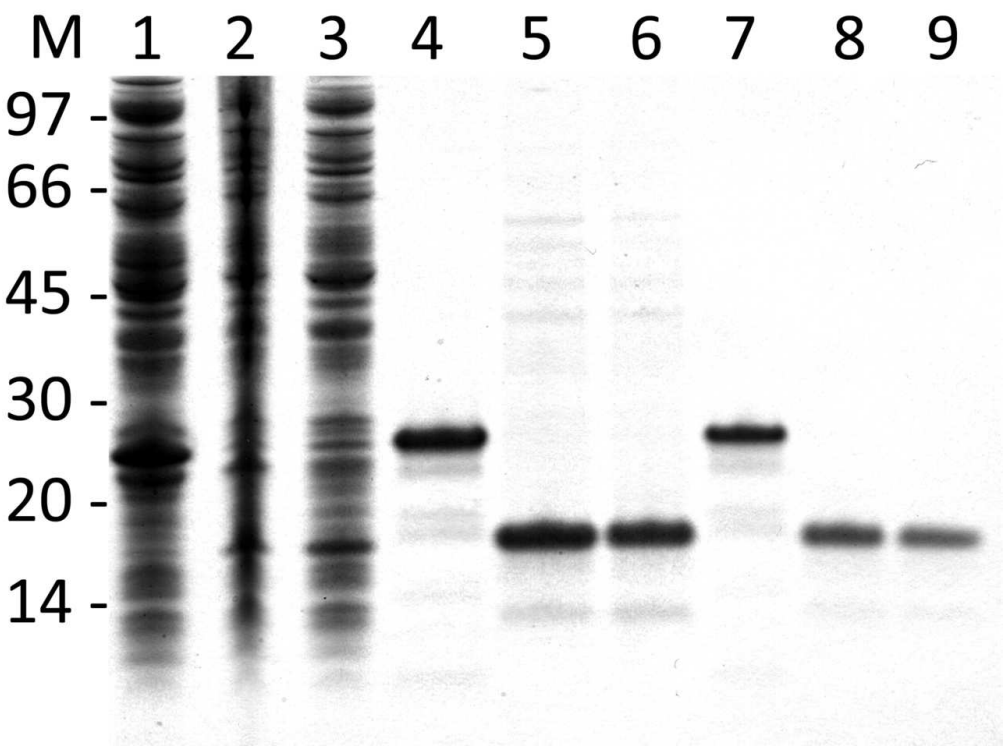

54x40mm (600 x 600 DPI)